Available online at www.sciencedirect.com
SCIENCE DIRECT®
Journal of Solid State Chemistry 174 (2003) 482–488
JOURNAL OF SOLID STATE CHEMISTRY
http://elsevier.com/locate/jssc

Effect of the Al/Si atomic ratio on surface and structural properties of sol–gel prepared aluminosilicates

V. La Parola,[a] G. Deganello,[a,b] S. Scirè,[c] and A.M. Venezia[b,*]

[a] *Dipartimento di Chimica Inorganica e di Chimica Analitica "Stanislao Cannizzaro" Università di Palermo, Viale delle Scienze, Parco D'Orleans 90128, Palermo, Italy*

[b] *Istituto per lo Studio dei Materiali Nanostrutturati, ISMN-CNR Sezione di Palermo, Via Ugo La Malfa 153, 90146, Palermo, Italy*

[c] *Dipartimento di Scienze Chimiche, Università di Catania, Catania, Viale A. Doria 6, 95125, Italy*

Received 20 December 2002; received in revised form 28 May 2003; accepted 30 May 2003

Abstract

A series of aluminosilicates with an Al/Si ratio ranging from 0 to ∞ (0 for pure silica and ∞ for pure alumina) was prepared by sol–gel process and characterized by surface and structure techniques. Aluminum tri*sec*butoxide and tetramethylorthosilicate were used as precursors for the sol–gel synthesis. The acidic properties of the oxides were studied by determination of the zero point charges, through mass titration method, and, for selected samples, by FT-IR spectroscopy of adsorbed pyridine used as a probe for both Brønsted and Lewis acidity. A dependence of the acidity on the Al/Si atomic ratio was found. According to the X-ray diffraction patterns, all the oxides have an amorphous structure except pure alumina exhibiting a γ-alumina pattern. The surface areas of the mixed oxides increase with increasing amount of alumina and are higher as compared to the individual oxides. The surface elemental distribution and electronic properties were investigated by X-ray photoelectron spectroscopy. According to the results, good agreement between the surface Al/Si atomic ratio and the analytical ratio is obtained.

Keywords: Silica-aluminas; Brønsted and Lewis acid; XPS; IR spectroscopy

1. Introduction

The availability of suitable supports for metal catalysts is of fundamental importance in heterogeneous catalysis. Due to its good textural and mechanical properties and its low cost, γ-alumina is one of the most used supports, especially in hydrotreating catalysis [1]. The chemical interaction between alumina and supported phases may contribute to the catalyst stability against sintering processes. Amorphous silica with its generally high surface area and high purity is also used as support [2]. However it generally leads to lower activity catalysts, and since it interacts less with the active species, allows detailed studies of catalysts characterization [3]. Mixed oxides such as amorphous silica aluminas (ASA) possess interesting properties especially when they are well mixed on a molecular scale. The combination of the two oxides may give rise to surface acid sites which are not present in either of the pure components [4]. The maximum acid strength of some mixed oxides was found to correlate with the average electronegativity of the cations [4–5]. Several models have been proposed to explain the appearance of the acid sites in a mixed oxide [6]. Following certain rules, once the excess of charge near the cation is calculated it follows that a positive charge is associated with Lewis acid sites, whereas excess negative charge is associated with Brønsted sites [5]. The surface acidity of the mixed oxides depends on the Al/Si atomic ratio [7]. The sol–gel chemistry allows to prepare mixed silica-alumina oxides with different Al/Si ratio and with well-defined surface areas, pore distribution and crystallinity [8]. However the attainment of a good molecular scale mixing is still a hard task [9]. The characteristics of the obtained oxides strongly depend on the sol–gel parameters such as the precursor molecules, their concentration, the solvent, the temperature, the amount of water of hydrolysis, and the pH [3–4]. Regarding the use of amorphous silica-aluminas as supports for

*Corresponding author. Fax: +390-916-809-399.
E-mail address: anna@pa.ismn.cnr.it (A.M. Venezia).

0022-4596/03/$ - see front matter © 2003 Elsevier Inc. All rights reserved.
doi:10.1016/S0022-4596(03)00321-9

hydrotreating catalysts [10–11], a dependence of the catalytic activity of the supported CoMo catalysts on the alumina/silica ratio and on the related acid–base properties was found [12]. Moreover the opposite effect of sodium ions added to pure silica and to a commercial amorphous aluminosilicate, on the hydrodesulfurization activity of CoMo catalysts, lead us to prepare in a controlled way a series of aluminosilicates with an Al/Si ratio ranging from 0 to ∞ (0 for pure silica and ∞ for pure alumina) in order to investigate in details the support effect in relation to its acidity and structural properties [10–13]. To this aim a series of aluminosilicates was prepared by sol–gel route and characterized by several techniques. The acidic properties of the oxides were studied by determination of the zero point charges (ZPC), through mass titration method, and, for selected samples, by IR spectroscopy of adsorbed pyridine used as a probe for both Brønsted and Lewis acidity. The surface and structural properties were studied by X-ray photoelectron spectroscopy and X-ray diffraction analyses. The morphology, in terms of surface areas, pore distribution and pore volume, was studied by N_2 physisorption.

2. Experimental

2.1. Preparation of the oxides by the sol–gel

All operations were performed under an atmosphere of pure argon. All chemicals (Aldrich Chemical Company Inc.) were of reagent grade purity and used as received. The required amounts of $Al(O\text{-}sec\text{-}Bu)_3$ and $Si(OEt)_4$ were mixed together. The solution was stirred for 3 h at room temperature under Ar flow in order to obtain a homogeneous mixture. The temperature was then raised to 353 K and the hydrolysis was performed by adding water (pH = 9 for ammonia) in stoichiometric amount to the rapidly stirred reaction mixture to allow the slow hydrolysis of the two alkoxides [4]. The hydrolysis in a basic environment should indeed promote formation of a mesoporous structure with less initial surface area as compared to samples prepared with acid hydrolysis, but more stable during heat treatment [4]. The gel, which formed in a few minutes, was left for 5 h under reflux and constant stirring. Then it was aged in air inside the flask for 5 days at room temperature. The colorless gel, homogeneous at visual inspection, was washed with sec butanol to remove possible traces of unhydrolyzed alkoxide. The washing fractions were completely clear on water addition. The xerogels were calcined in air at 773 K overnight. The list of prepared supports is given in Table 1. The nominal Al/Si atomic ratio corresponded to the bulk ratio as confirmed from the X-ray fluorescence analyses. In order to check the reproducibility of the preparation method, the syntheses of supports with the same Al/Si ratios were repeated at least twice.

Table 1
Al/Si bulk (nominal) and XPS derived atomic ratios, surface areas and zero point charges. In parentheses the atomic ratios obtained considering only the Si 2*p* component at high energy are reported

Samples	$Al/Si_{(bulk)}$	$Al/Si_{(XPS)}$	S (m^2/g)	Z.P.C
*s*AlO	∞	∞	210	n.d.
*s*3	3.50	2.46 (3.23)	480	6.4
*s*2	2.34	1.85 (2.28)	488	5.6
*s*1	1.18	1.11 (1.22)	450	4.5
*s*0.3	0.39	0.30 (0.31)	355	4.1
*s*0.17	0.18	0.11	150	3.7
*s*0	0	0	143	5.2

2.2. Catalyst characterization

2.2.1. Zero point charge

The zero point charge of the supports was determined by mass titration [14]. According to this method, the variation of pH of a water solution containing increasing amount of solid was monitored until the steady state value of pH (ZPC) was reached.

2.2.2. IR spectroscopy

IR spectra were recorded with a Perkin Elmer System 2000 FT-IR spectrophotometer with a resolution of $2\,cm^{-1}$. The powdered samples were compressed into thin self-supporting discs of about $25\,mg\,cm^{-2}$ and 0.1 mm thick. The disc was placed in an IR cell which allows thermal treatments in vacuum or in a controlled atmosphere. In the cell all samples were evacuated at 400°C for 1 h and finally cooled at room temperature. Pyridine was then admitted by opening for some seconds the valve of the vessel containing the substance at 283 K. Subsequent evacuations were then performed at 423 K. Data are reported as difference spectra obtained by subtracting the spectrum of the sample before the admission of pyridine and are normalized to the same amount of catalysts per cm^2.

2.2.3. X-ray diffraction

X-ray diffraction measurements for the structure determination were carried out with a Philips vertical goniometer using Ni-filtered Cu$K\alpha$ radiation. A proportional counter and 0.05° step sizes in 2θ were used.

2.2.4. BET analyses

The microstructural characterization was performed with a Carlo Erba Sorptomat 1900 instrument. The fully computerized analysis of the adsorption isotherm of nitrogen at liquid nitrogen temperature, allowed obtaining, through the BET approach, the specific surface area of the samples. By analysis of the desorption curve,

using the Dollimore and Heal calculation method, the pore size volume distribution was also obtained [15].

2.2.5. XPS

The X-ray photoelectron spectroscopy analyses were performed with a VG Microtech ESCA 3000 Multilab, equipped with a dual Mg/Al anode. The spectra were excited by the non-monochromatized Al$K\alpha$ source (1486.6 eV) run at 14 kV and 15 mA. The analyzer operated in the constant analyzer energy (CAE) mode. For the individual peak energy regions, a pass energy of 20 eV set across the hemispheres was used. Survey spectra were measured at 50 eV pass energy. The sample powders were analyzed as pellets, mounted on a double-sided adhesive tape. The pressure in the analysis chamber was in the range of 10^{-8} Torr during data collection. The constant charging of the samples was removed by referencing all the energies to the C 1*s* set at 285.1 eV, arising from the adventitious carbon. The invariance of the peak shapes and widths at the beginning and at the end of the analyses ensured absence of differential charging. Analyses of the peaks were performed with the software provided by VG, based on non-linear least-squares fitting program using a properly weighted sum of Lorentzian and Gaussian component curves after background subtraction according to Shirley and Sherwood [16–17]. Atomic concentrations were calculated from integral intensity of the chosen peaks using ionization cross sections provided by the instrument software. The binding energy (BE) values are quoted with a precision of ± 0.15 eV.

2.3. Results and discussion

The oxides with different Al/Si overall ratios are listed in Table 1 along with the surface ratios as found by XPS, the surface area and the zero point charge. The ZPC or IEPS (isoelectric point) is an important property in the design of oxide supported catalysts since it determines the adsorption features of the different oxides as function of the pH of the impregnating solution [18]. The ZPC is a measure of the polarizability of the material which tends to be surface charged once suspended in aqueous solution. The surface charge, being neutralized by adsorption of OH^- or H^+ is a measurements of the total surface acidity of the solid. As can be observed in the table, the ZPC increases with the increase of the amount of alumina in the mixed oxides. The ZPC value of sol–gel prepared silica is higher as compared to the values in Ref. [18]. Differences are likely to be due to the preparation method and to the presence of structural defects.

Oxide surfaces exhibit both Brønsted and Lewis acidity. The Brønsted acid sites arise from silanol groups which can be generated when a trivalent cation, like Al^{3+}, is present in tetrahedral coordination with oxygen. When the oxygen anions are shared between the cations, net negative charges are created on aluminum and are compensated by protons giving rise to terminal silanol groups and to the more acidic bridging hydroxyl groups. The Lewis acidity arises from partly uncoordinated metal cations and anions present at the surface of metal oxides which with water (always present in the environment) produce surface hydroxy-groups [19]. They are also formed through the isomorphous substitution of Si^{4+} lattice sites by Al^{3+} ions. In pure silica, characterized by covalent Si–O bonding, Brønsted acidity is low and Lewis sites are absent unless silica has been activated at very high temperatures [19–20]. A study of the surface acidity may be done by using a basic molecule, such as pyridine, as a probe which interacts through the electronic lone pair of its N atom with sites of different acidity and is able to probe both Lewis and Brønsted acidity [21]. This interaction is studied by IR spectroscopy. The stretching vibrations $\nu_{8a,b}$ and $\nu_{19a,b}$ of the pyridine ring are the most sensitive modes used in IR studies to evaluate the strength of the adsorptive interaction. Generally the bands at ca. 1640 and 1540 cm^{-1} are characteristics of pyridinium ions (adsorption of pyridine on Brønsted sites), whereas bands in the region 1600–1630 cm^{-1} and 1440–1455 cm^{-1}, are attributed to coordinately adsorbed pyridine on Lewis sites [19]. The band at 1492 cm^{-1} is less informative, being associated with both Brønsted and Lewis site. While the frequencies of the bands of pyridinium do not change substantially upon varying the acidity of the solid, the bands related to coordinatively bound pyridine move to high frequency as the strength of interaction increases, the ν_{8a} band being more sensitive. In Fig. 1a the FT-IR spectra in the region 1700–1400 cm^{-1} over three silica-alumina samples, after admission of pyridine and subsequent evacuation at 423 K to eliminate the physisorbed pyridine, are shown. The *s*3 sample exhibits a spectrum which is typical of the adsorption of pyridine on Lewis acid sites. The main features of the spectrum are the ν_{19b} band at 1452 cm^{-1} and the ν_{8a} band at 1625 cm^{-1}. Very weak bands at ca. 1540 and 1640 cm^{-1} can be also noted, indicating the presence of a very low amount of Brønsted acid sites on the catalytic surface of this sample. Therefore it is evident from the figure that the *s*3 sample has considerable Lewis but very low Brønsted acidity. On *s*03 and *s*1 samples the peaks characteristics of pyridinium ions are more intense, clearly indicating that the two samples present a higher Brønsted acidity compared to that of the alumina rich sample *s*3. The intensity ratio between the peak at 1640 cm^{-1} and the one at 1625 cm^{-1} seems to indicate that in *s*0.3 the ratio of the Brønsted sites to Lewis sites is larger than in *s*1. As indicated by the invariance of the peak positions among the three considered samples, the acid sites have similar strength. Based on the results, concerning the

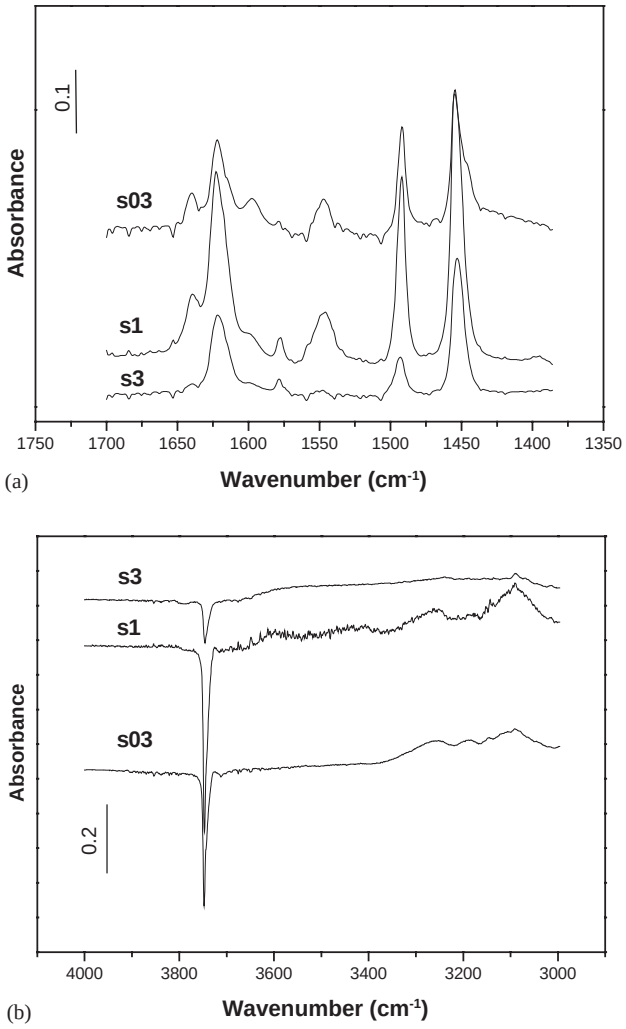

Fig. 1. FT-IR spectra of selected silica-alumina samples after admission of pyridine and subsequent outgassing at 423 K. Data are reported as difference spectra obtained by subtracting the spectrum of the sample before the admission of pyridine.

Lewis/Brønsted acidity ratio, the following order $s3 > s1 > s03$ is obtained. Such acidity order is in accord with the rules formulated by Tanabe [5–6]. Following these rules, the excess of positive charge, calculated for the aluminum rich oxides, is associated with Lewis acid sites whereas the excess of negative charge in the silica enriched oxides, is associated with Brønsted sites [6]. In Fig. 1b, in which the FT-IR spectra in the region 4000–3000 cm^{-1} after admission of pyridine and subsequent evacuation at 423 K are shown, it is possible to observe that pyridine adsorption brings about the decrease of the OH stretching band at 3746 cm^{-1} (strong negative peak), characteristic of the silanol band observed in pure silica [22]. However at a careful inspection of the band, an asymmetry at lower frequency (3742 cm^{-1}) is observed. In accord with literature [23] this feature may be attributed to the more acidic bridging hydroxyl groups able to form the pyridinium ion, as detected in Fig. 1a. There is no evidence of alumina-like hydroxyl bands.

For all the analyzed samples, the N_2 adsorption curves in the low-pressure region conformed to the BET Type II isotherm, whereas in the higher-pressure region the hysteresis loop typical of mesoporous materials appeared. The specific surface areas obtained from the BET method are listed in Table 1. The areas of the mixed oxides are larger as compared to the single oxides. Moreover the surface area decreases with the increase of silica amount. This result differs from the one obtained for mixed alumina-silica oxides prepared by sol–gel, using different precursors and different preparation steps [24]. In that case a decrease of the surface area with increase of alumina content was found [24]. In Fig. 2 the pore distributions of the silica-alumina oxides are shown. All of the samples have mesopores. The oxides with high alumina content, like *s*AlO, *s*3 and *s*2, exhibit a pore distribution centered at the low size end of the mesopore region, the mixed oxides with high silica content, *s*0.3 and *s*0.17, have larger pores. As mentioned in the experimental part, sol hydrolysis in basic environment may have promoted formation of mesoporous structure [4].

The X-ray diffractograms of the mixed oxides after calcinations at 773 K are shown in Fig. 3. Pure silica and pure alumina show features typical of amorphous silica and of γ-alumina with contribution from a distorted θ-alumina respectively, while all the other diffractograms are typical of amorphous aluminosilicates. The amorphism of the obtained silica-alumina systems is generally indicative of a well-mixed two component oxide [25].

The XPS survey spectra of the samples evidenced only oxygen, silicon, aluminum and carbon peaks. The binding energy of Al 2*p*, Si 2*p* and O 1*s* peaks with the relative full-width at half-maximum (FWHM) are summarized in Table 2. Silicon and oxygen are strongly affected by the presence of aluminum; the binding energy of these peaks decreases with increasing aluminum content and for all samples the difference between the two energies, Δ[O(1*s*)–Si(2*p*)], considering the high energy Si 2*p* component, is equal to 429 eV. As reported

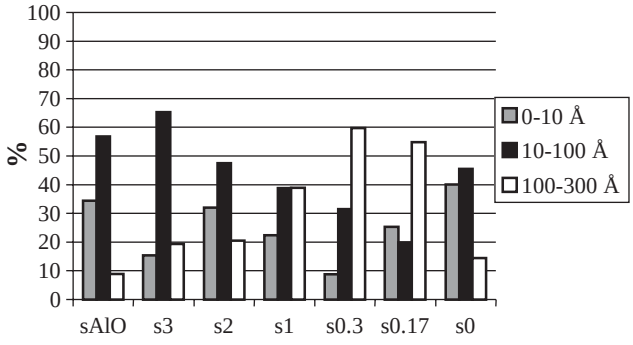

Fig. 2. Pore distribution of the silica-alumina oxides.

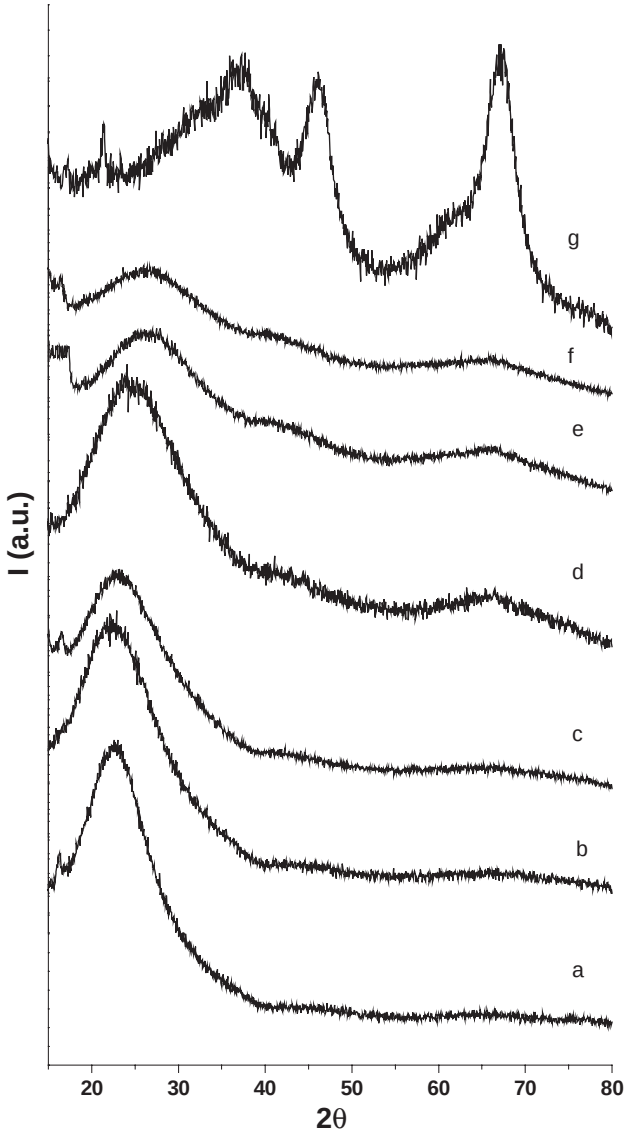

Fig. 3. X-ray diffractograms of the oxides. (a) *s*0, (b) *s*0.17, (c) *s*0.3, (d) *s*1, (e) *s*2, (f) *s*3 and (g) *s*AlO.

for zeolites and pumice, which is a natural amorphous aluminosilicate with composition similar to *s*0.17, the binding energies of all the elements, especially of silicon and oxygen, shift in the same direction [26]. This can be explained by assuming the presence of group units rather than elemental units in which the silica framework acts as the cation like unit and the alumina framework as anion [26–27]. As more Al–O units are inserted into a silica type framework, the binding energy of the Si (2*p*) peak progressively decreases to reflect the enhanced covalency induced into the Si–O bonds by the more ionic Al–O units [28]. The aluminum binding energy is less affected by the presence of silicon, its binding energy ranging between 74.6 eV from pure alumina to 75.2 eV for the highest Al/Si ratio oxide compound. Analogously to the aluminosilicate sodalite and zeolite Na-*A*, the increase of both Al 2*p* and Si 2*p*

Table 2
Al 2*p*, Si 2*p* and O 1*s* binding energies (eV) of the oxides with the FWHM in parentheses. For silicon and oxygen the relative percentage of each chemical species are reported

Samples	Al 2*p*	Si 2*p*	Relat. Si (%)	O 1*s*	Relat. O (%)
*s*AlO	74.7 (1.9)			531.1 (2.2)	
*s*3	74.7 (2.4)	100.0 (2.5)	23.6	531.3 (2.7)	80.8
		102.3 (2.5)	76.4	533.0 (2.7)	19.2
*s*2	74.6 (2.8)	99.5 (2.8)	18.9	531.1 (3.2)	
		102.2 (2.8)	81.1		
*s*1	75.1 (2.4)	100.6 (2.5)	9.0	531.8 (2.8)	
		102.8 (2.5)	91.0		
*s*0.3	75.3 (2.5)	100. 3 (2.6)	3.0	532.3 (2.8)	
		103.3 (2.6)	97.0		
*s*0.17	75.2 (2.6)	100.4 (2.6)	1.7	532.3 (2.8)	
		103.5 (2.6)	98.3		
*s*0	–	103.9 (2.3)	100	532.9 (2.4)	

binding energies with the decrease of the Al/Si ratio, is indicative of aluminate units located in tetrahedral environments, substituting some of the silicate units [28]. The nearly constant FWHMs obtained along the series of samples are a good indication of sample homogeneity. As it can be observed in Fig. 4, the Si 2*p* region presents an additional component at lower binding energy whose intensity increases with the increasing of alumina in the oxides. This feature lies at binding energy around 100 eV and is present in all samples, except pure silica, in different percentage. Its binding energy is typical for silicon in reduced state [29]. In Table 1 the bulk atomic ratio Al/Si, corresponding to the analytical sample composition, and the surface ratio as derived from XPS peak areas are also reported. The XPS data reported in column 3 refer to the total Si 2*p* intensity. In the same column, the values in parentheses represent the atomic ratios as obtained considering only the high energy component of the Si 2*p* peak. Bulk ratios slightly differ from the XPS ratios calculated with the total Si 2*p* areas. Contrary to XPS results on similar oxides, showing quite large discrepancy between the bulk and the surface composition, here the deviation is not very pronounced, and if we use only the silicon component at high binding energy, (see values in parentheses) the Al/Si ratio becomes close to the nominal [30]. In order to verify that the component at ca. 100 eV is indeed a surface species with a lower oxidation state due to surface distortion phenomena, angular variation measurements were carried out. If the Si reduced component was a surface species, its XPS intensity relative to the intensity of the oxidized species would increase with the increasing of the surface sensitivity. The study was made on the selected sample, *s*2. By decreasing the take off angle, considered with respect to the sample surface, therefore enhancing the surface sensitivity, a small but continuous increase of the Si $2p_{red}$ component relative to Si $2p_{ox}$ component

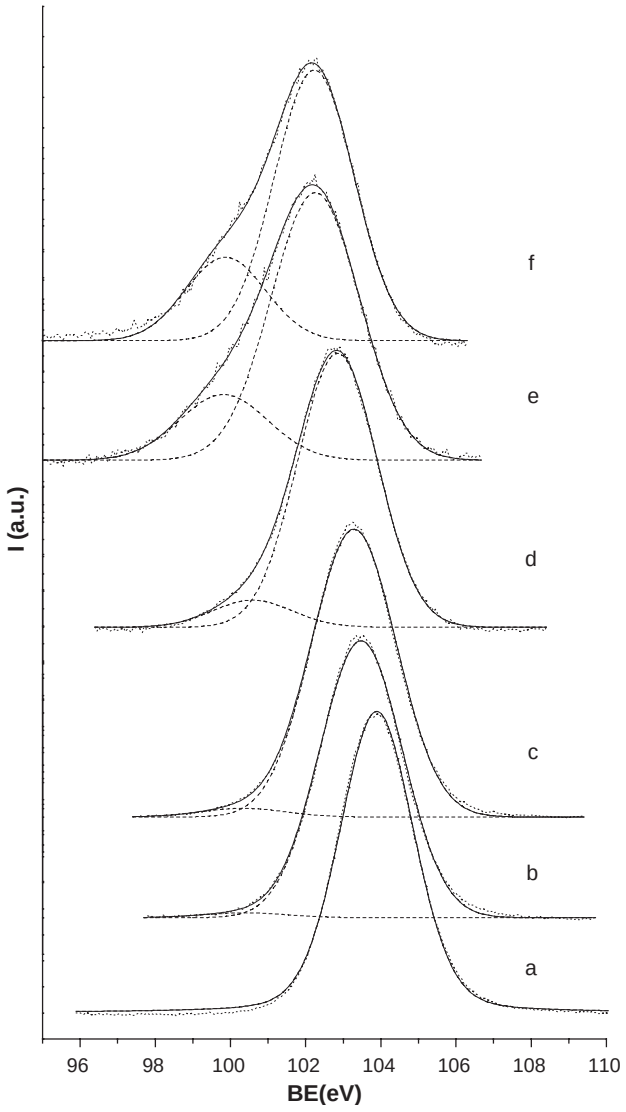

Fig. 4. Si 2*p* spectra of the oxides. (a) *s*0, (b) *s*0.17, (c) *s*0.3, (d) *s*1, (e) *s*2, and (f) *s*3. Dotted line: experimental data; solid line: fitted data; dashed line: fitted components.

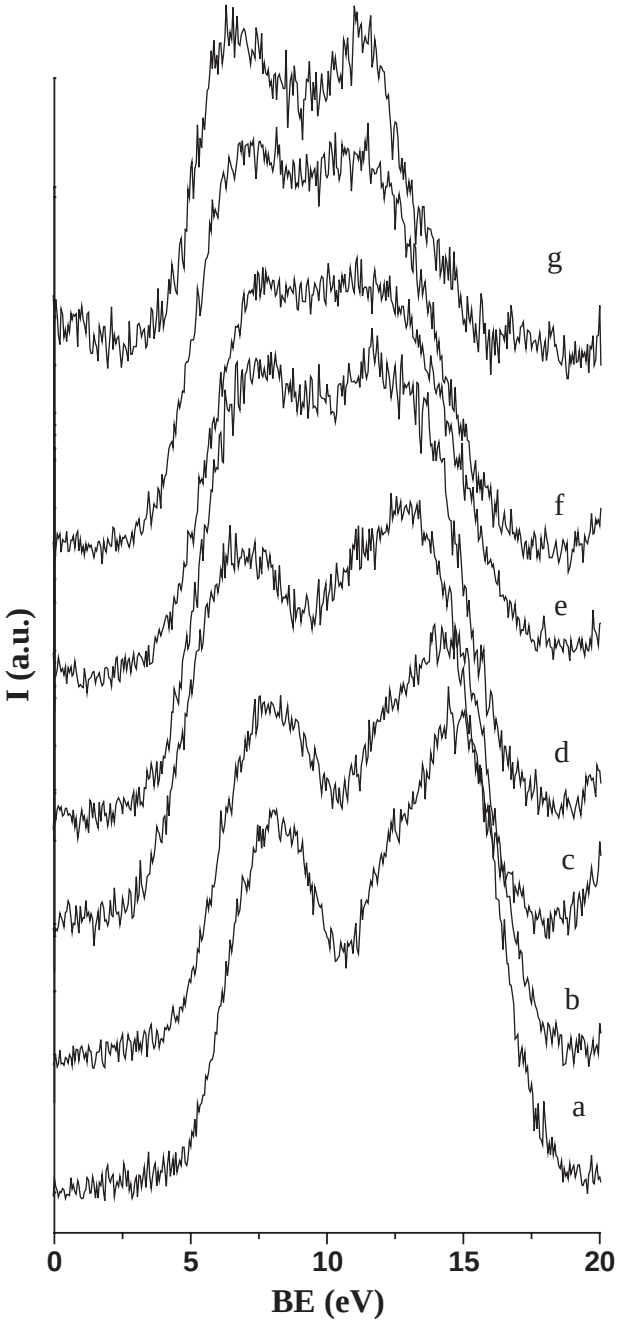

Fig. 5. Valence region of the oxides (a) *s*0, (b) *s*0.17, (c) *s*0.3, (d) *s*1, (e) *s*2, and (f) *s*3, (g) *s*AlO.

was observed. At the same time a decrease of the total Al 2*p* over Si 2*p* intensity ratio was also obtained. It can be concluded that, as also described in the literature for zeolites and other aluminosilicate a surface layer enriched in Si is formed [26,29].

The X-ray induced valence spectra of the alumina-silica oxides were also studied in the range 0–20 eV, and the relative spectra are shown in Fig. 5. The valence region changes with the relative percentage of the two oxides. The spectrum of pure silica (Fig. 5a) is rather broad (ca. 15 eV) and is divided into two substructures. The one centered at 8.1 eV is mainly due to O 2*p* non-bonding orbitals. The second substructure is quite broad and is divided into two sub-bands. One centered at 12.1 eV and due to bonding orbitals formed from O 2*p* and Si 3*p* and the other one at 14.9 eV due to bonding orbitals formed from O 2*p* and Si 3*s* [31]. The gulf between the two substructures is the bonding "barrier" and is a measure of the covalent character; the deeper is the gap the greater is the covalency. The spectrum of pure alumina is narrower than the silica one (ca. 9 eV) and again two sub-bands are observed; one centered at 6.6 eV due to the non-bonding O 2*p* orbitals and the other centered at 11 eV due to the bonding orbitals (O 2*p* and Al 2*p* or Al 2*s*). The gap between these two bands is rather shallow, indicating that alumina has less covalent bonding stabilization than silica with a larger degree of

ionicity [31]. The spectra of the low Al/Si ratio compounds are different from the corresponding spectra of zeolite with similar composition which are characterized by three different regions, they rather resemble the valence band of the amorphous natural pumice [27,31]. The shape of the band remains similar to the pure silica band in the mixed oxide with low Al/Si atomic ratio (up to the *s*0.3 sample) even though there is a downwards binding energy shift and a modification of the relative intensities of the two main substructures. These changes are in accord with the structure of silica slightly perturbed by aluminate ions. By increasing the alumina content the valence spectra resemble more closely the alumina one. The peak due to the non-bonding O 2*p* orbital moves down to 6.6 eV and the peak due to the bonding orbitals move to 11 eV. Moreover, the relative intensity of the two substructures inverts, and the gap becomes shallow.

3. Conclusion

To summarize, the synthesis sol–gel adopted in this study afforded the preparation of mixed silica-alumina oxides. The mixed oxides exhibited amorphous diffractogram, differently from the pure alumina sample characterized by the γ-Al_2O_3 phase. The lack of crystallinity even in the alumina rich samples was an indication of good molecular mixing. As shown by the IR spectra of adsorbed pyridine on three selected samples, Lewis acid sites of similar strength are present on the surface of the mixed oxides independently on the Al/Si atomic ratio. On the contrary, the Brønsted acid sites are formed essentially in the samples with higher percentage of silica. The region of the hydroxyl groups is characterized by an asymmetric band likely due to terminal silanol and bridging hydroxyl groups. From the quantitative XPS analyses, Al/Si atomic ratios in good agreement with the overall bulk ratios were obtained. A slight surface segregation of a species containing silicon in a reduced electronic state was also found. Such surface species was not detected on pure silica and therefore it seemed to be induced by the presence of alumina. Also indicative of good molecular mixing was the gradual variation of the structure of the valence spectra of the oxides, from the pure silica spectrum, characterized by a deep gap between two substructures, indicative of covalent Si–O bonding, to the pure alumina spectrum characterized by shallower gap, typical of larger degree of ionicity of the Al–O bond.

References

[1] H. Topsøe, B.S. Clausen, F.E. Massoth, in: J.R. Anderson, M. Boudart (Eds.), Hydrotreating Catalysis, Springer, Berlin, 1996.
[2] R. Voyatiz, J.B. Moffat, J. Catal. 142 (1993) 45.
[3] M. Breysse, J.L. Portefaix, M. Vrinat, Catal. Today 10 (1991) 489.
[4] J.B. Miller, I.E. Ko, Catal. Today 35 (1997) 269.
[5] K. Shibata, T. Kiyoura, J. Kitagawa, T. Sumiyoshi, K. Tanabe, Bull. Chem. Soc. Jpn. 46 (1973) 2985.
[6] K. Tanabe, T. Sumiyoshi, K. Shibata, T. Kiyoura, J. Kitagawa, Bull. Chem Soc. Jpn. 47 (5) (1974) 1064.
[7] R.G. Lelived, T.G. Ros, A.J. van Dillen, J.W. Geus, D.C. Koningsberger, J. Catal. 185 (1999) 513.
[8] J. Livage, M. Henry, C. Sanchez, Prog. Solid State Chem. 18 (1988) 259.
[9] C. Sârbu, B. Delmon, Appl. Catal. A 185 (1999) 85.
[10] A.M. Venezia, F. Raimondi, V. La Parola, G. Deganello, J. Catal. 194 (2000) 393.
[11] R. Navarro, B. Pawelec, J.L.G. Fierro, P.T. Vasudevan, Recent. Res. Dev. Catal. (1996) 1.
[12] A.M Venezia, V. La Parola, G. Deganello, GIC 2000, 1–5 Ottobre 2000, Ravello, Italia.
[13] A.M. Venezia, V. La Parola, G. Deganello, D. Cauzzi, G. Leonardi, G. Predieri, Appl. Catal. A 229 (2002) 261.
[14] S. Subramanian, J.S. Noh, J.A. Schwarz, J. Catal. 114 (1988) 433.
[15] S.J. Gregg, K.S. Sing, Adsorption Surface Area and Porosity, 2nd Edition, Academic Press, San Diego, 1982.
[16] D.A. Shirley, Phys. Rev. B 5 (1972) 4709.
[17] P.M.A. Sherwood, in: D. Briggs, M.P. Seah (Eds.), Practical Surface Analysis, Wiley, New York, 1990, p. 181.
[18] J.P. Brunelle, Pure Appl. Chem. 50 (1978) 1211.
[19] G. Busca, Catal. Today 41 (1998) 191.
[20] B.A. Morrow, I.A. Cody, J. Phys. Chem. 80 (1976) 1998.
[21] H. Knozinger, Adv. Catal. 25 (1976) 184.
[22] T.B. Beebe, P. Gelin, J.T. Yates, Surf. Sci. 148 (1984) 526.
[23] M. Trombetta, G. Busca, S. Rossini, V. Piccoli, U. Corsaro, A. Guercio, R. Catani, R.J. Willey, J. Catal. 179 (1998) 581.
[24] T.J. Bandosz, C. Lin, J.A. Ritter, J. Colloid Interface Sci. 198 (1998) 347.
[25] M. Schraml-Marth, K.L. Walther, A. Wokaun, B.E. Handy, A. Baiker, J. Non-Cryst. Solids 143 (1992) 1.
[26] T. Barr, M.A. Lishka, J. Am. Chem. Soc. 108 (1986) 3178.
[27] A.M. Venezia, M.A. Floriano, G. Deganello, A. Rossi, Surf. Interface Anal. 18 (1992) 532.
[28] B. Herreros, H. He, T.L. Barr, J. Klinowski, J. Phys. Chem 98 (1994) 1302.
[29] T.L. Barr, Appl. Surf. Sci. 15 (1983) 1.
[30] W. Daniell, U. Schubert, R. Glöckler, A. Meyer, K. Noweck, H. Knözinger, Appl. Catal. A General 196 (2000) 247.
[31] T.L. Barr, L.M. Chen, M. Mohsenian, M.A. Lishka, J. Am. Chem. Soc. 110 (1988) 7962.